Alloy Nanoclusters

International Edition: DOI: 10.1002/anie.201509381
German Edition: DOI: 10.1002/ange.201509381

Templated Atom-Precise Galvanic Synthesis and Structure Elucidation of a $[Ag_{24}Au(SR)_{18}]^-$ Nanocluster

*Megalamane S. Bootharaju, Chakra P. Joshi, Manas R. Parida, Omar F. Mohammed, and Osman M. Bakr**

Abstract: *Synthesis of atom-precise alloy nanoclusters with uniform composition is challenging when the alloying atoms are similar in size (for example, Ag and Au). A galvanic exchange strategy has been devised to produce a compositionally uniform $[Ag_{24}Au(SR)_{18}]^-$ cluster (SR: thiolate) using a pure $[Ag_{25}(SR)_{18}]^-$ cluster as a template. Conversely, the direct synthesis of $Ag_{24}Au$ cluster leads to a mixture of $[Ag_{25-x}Au_x(SR)_{18}]^-$, $x = 1$–8. Mass spectrometry and crystallography of $[Ag_{24}Au(SR)_{18}]^-$ reveal the presence of the Au heteroatom at the Ag_{25} center, forming $Ag_{24}Au$. The successful exchange of the central Ag of Ag_{25} with Au causes perturbations in the Ag_{25} crystal structure, which are reflected in the absorption, luminescence, and ambient stability of the particle. These properties are compared with those of Ag_{25} and $Ag_{24}Pd$ clusters with same ligand and structural framework, providing new insights into the modulation of cluster properties with dopants at the single-atom level.*

Atomically precise nanoparticles, or nanoclusters, have received significant attention over the past decade.[1] This special class of nanomaterials, which has sizes in between those of atoms and plasmonic nanoparticles, exhibits dual characteristics[2] and unusual physicochemical[1d,3] properties due to the confinement of the electrons. To date, a large number of monothiolated gold clusters have been synthesized and crystallized,[4] while just two purely monothiolated silver clusters, Ag_{44}[5] and Ag_{25},[2] have been fully characterized. Among the many Au clusters, $Au_{25}(SR)_{18}$ has been the most extensively studied[4] owing to its utility as a model system. In contrast, its highly sought after silver counterpart, $Ag_{25}(SR)_{18}$, was reported[2] only recently.

Alloy nanoparticles and nanoclusters are attractive for certain applications owing to their synergistic and enhanced properties compared to their homometallic analogues.[5a,6] Heteroatom substitution of homometal nanoclusters causes significant changes in particle stability,[7] luminescence,[8] catalytic activity,[9] ligand-exchange reactivity,[10] electronic,[11] and electrochemical[12] properties. Hence, there is an essential need for nanoparticles systems and approaches that enable the investigation of doping and alloying at the single-atom level.

Recently, significant efforts have been devoted to developing alloy clusters.[6b] For instance, $Au_{25}(SR)_{18}$ was doped with various metals, such as Hg,[13] Cd,[14] Pt,[9] Pd,[7] Cu,[15] and Ag;[11,16] only the first two cases resulted in monodisperse alloy clusters, while others produced a mixture of clusters that were subsequently purified. In silver, only Pt and Pd (different atomic size from Ag) have been successfully implemented to obtain atomically and compositionally precise Ag clusters $[Ag_{24}M_1(SR)_{18}]^{2-}$ (M = Pd, Pt).[17] In contrast, atomically precise doping of Ag nanoclusters with similar sized atoms such as Au and vice versa results in a distribution of compositions,[5a,11,16] with only some parts of the sample crystallizing.[16] While the crystallized components have provided important insights into the structure and possible positions of the dopant,[5a,16] they are not representative of the nanocluster properties as a whole. The similar sizes of Ag and Au (atomic radii ca. 1.44 Å) render it problematic to control the amount of dopant in a cluster, thus producing distributions of alloy compositions that are tough to purify.

In this study, we demonstrate the atomically precise doping of a silver cluster by gold through a novel galvanic exchange strategy. Through this strategy we obtain a pure $[Ag_{24}Au(SR)_{18}]^-$ cluster. In contrast, we show that a direct synthesis of such a cluster produces a mixture of AgAu alloy clusters, which is ill-defined in composition. Only through developing controlled atom-precise galvanic exchange were we able to crystallize and determine the total structure of the $[Ag_{24}Au(SR)_{18}]^-$ cluster. In comparison to $[Ag_{25}(SR)_{18}]^-$, $[Ag_{24}Au(SR)_{18}]^-$ exhibits enhanced stability, as well as photoluminescence and excited-state lifetimes. $[Ag_{25}(SR)_{18}]^-$ is so far the only family of Ag clusters that has an analogous set of atomically pure, centrally substituted heteroatom (that is, $Ag_{25}(SR)_{18}$, $Ag_{24}Au(SR)_{18}$, and $Ag_{24}Pd(SR)_{18}$). This unique set of model clusters makes it possible to study the effects of atomic substitution on the electronic structure, stability, and photophysical properties of Ag clusters.

Attempts to synthesize the target alloy cluster $Ag_{24}Au(SPhMe_2)_{18}$ through a direct reduction of the Ag and Au precursors in the presence of the $HSPhMe_2$ (2,4-dimethylbenzenethiol) (see the Supporting Information for details) produced a mixture of compositions with the same nominal structural framework. Electrospray ionization mass spectrometry (ESI MS) revealed the synthetic product as a mixture of $[Ag_{25-x}Au_x(SPhMe_2)_{18}]^-$ clusters ($x = 1$–8) (Supporting Information, Figure S1). Varying the incoming Au^+ concentration during synthesis did not yield a single pure cluster. The

[*] Dr. M. S. Bootharaju, C. P. Joshi, Dr. M. R. Parida, Prof. O. F. Mohammed, Prof. O. M. Bakr
Division of Physical Sciences and Engineering, Solar and Photovoltaics Engineering Research Center (SPERC), King Abdullah University of Science and Technology (KAUST)
Thuwal 23955-6900 (Saudi Arabia)
E-mail: osman.bakr@kaust.edu.sa

Supporting information for this article (synthesis and characterization details of Ag_{25}, $Ag_{24}Au$, $Ag_{24}Pd$, and $Ag_{25-x}Au_x$ clusters and single-crystal data of $Ag_{24}Au$) is available on the WWW under http://dx.doi.org/10.1002/anie.201509381.

optical spectra (Figure S1 inset) of these mixtures of clusters revealed the continuous modulation of Ag_{25} optical properties with the increase in dopant amount. This optical modulation is an average of many clusters, which we were unable to separate into individual species.

To achieve the formation of a pure $Ag_{24}Au(SPhMe_2)_{18}$ cluster, we reasoned that an approach that affords the slow and controllable introduction of heteroatoms would be needed. We thus designed a method that uses the $Ag_{25}(SPhMe_2)_{18}$ nanocluster as a starting molecular template (see the Supporting Information), while the controlled dopant incorporation is initiated by post-synthetic galvanic replacement of Ag atoms of cluster with Au atoms, resulting in atom-precise alloying. Au^+ ions, owing to their electrochemical potential difference with Ag atoms of Ag_{25}, were reduced to Au by Ag_{25}, producing Au-doped Ag_{25} clusters. ESI MS of a Ag_{25} control and its Au-doped equivalent cluster are compared in Figure 1. An intense peak at about m/z 5167

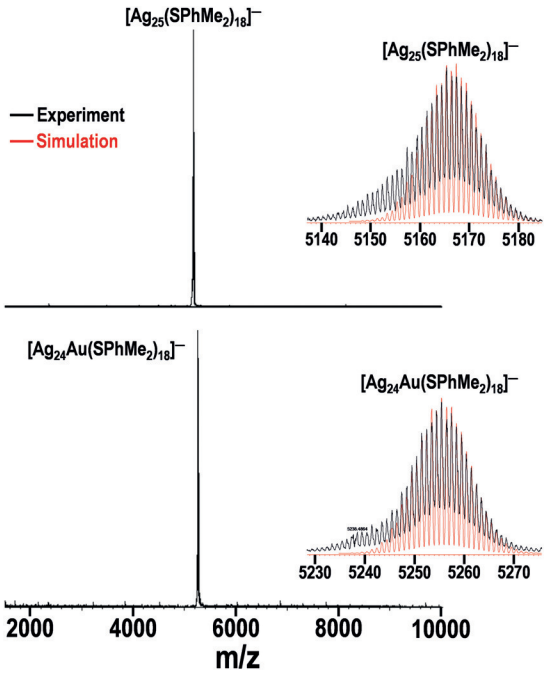

Figure 1. Negative-mode ESI MS of $[Ag_{25}(SPhMe_2)_{18}]^-$ and its galvanic exchange product with Au^+, namely the $[Ag_{24}Au(SPhMe_2)_{18}]^-$ cluster. Insets: experimental and simulated mass spectra of corresponding clusters.

corresponding to pure $Ag_{25}(SPhMe_2)_{18}$ is apparent. The excellent match of the simulated mass spectrum with the experiment confirms the assignment (Figure 1 inset). Similarly, the Au-doped cluster obtained by galvanic reduction exhibited only a single prominent peak, which appears at about m/z 5257. Magnification of this peak (Figure 1 inset) shows a characteristic isotopic pattern of silver with peaks separated by m/z 1, indicating that the cluster has a 1− core charge because the $HSPhMe_2$ ligand does not have any charged functional groups such as $-COO^-H^+$.[18] The mass difference of 90 between the m/z 5257 peak and that of the pure $Ag_{25}(SPhMe_2)_{18}$ is a clear indicator of the successful replacement of one Ag atom of Ag_{25} with one Au atom. This exchange was further confirmed by the exact match between the simulated spectrum of $[Ag_{24}Au(SPhMe_2)_{18}]^-$ and the experiment (Figure 1 inset). We note that the Ag atom that was expelled from Ag_{25} and replaced with Au during galvanic reaction was found to react with Cl^- from the Au precursor ($AuClPPh_3$), forming AgCl (Supporting Information, Figure S2) as a byproduct, which was discarded. The appearance of AgCl as a reaction byproduct further corroborates the proposed galvanic exchange method.

We note that there are only three possible locations in Ag_{25} for the dopant: the center, the surface of an icosahedron, or the ligand motifs of Ag_{25}. While ESI MS data show the successful formation of an atomically precise composition, the position of the inserted Au atom within the Ag_{25} structure entails the total structure elucidation by some other means. Therefore, we crystallized Au-doped clusters by the layering method (see the Supporting Information). The pure nature of the alloy product obtained by our galvanic exchange route facilitated the formation of high-quality single-crystals, which made it possible to study the cluster single-crystal X-ray diffraction (XRD).

The X-ray crystal structure of $Ag_{24}Au(SPhMe_2)_{18}$ (Supporting Information, Figures S3–S6 and Table S1) revealed the presence of a sole PPh_4^+ cation per cluster, confirming the proposed deduction from ESI MS that the clusters carry a unit negative charge. Further analysis of the crystal structure shows an arrangement of 12 Ag atoms that formed an icosahedron core with one Au atom at its center (Figure 2).

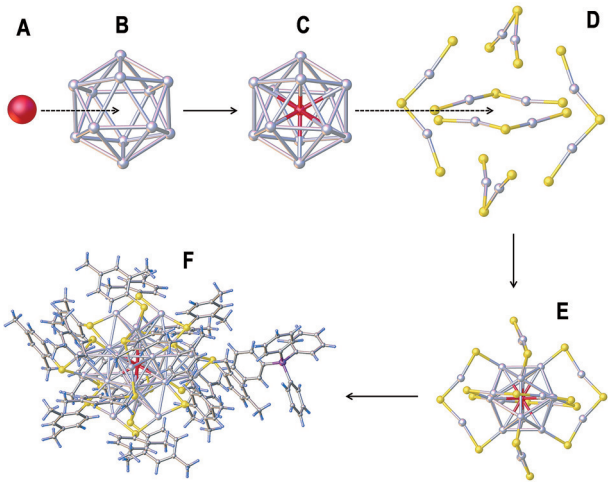

Figure 2. X-ray structure of $[Ag_{24}Au(SPhMe_2)_{18}]^-PPh_4^+$. A) Au atom; B) Ag_{12} icosahedron; C) Ag_{12} with central Au forming $Ag_{12}Au$ core; D) six V shaped Ag_2S_3 units; E) capping $Ag_{12}Au$ core with six Ag_2S_3 units; and F) the total structure of $Ag_{24}Au$ with counterion. Au red, Ag silver white, S yellow, P purple, C gray.[19]

The remaining 12 Ag atoms are shown to occupy the 12 triangular faces of the $Ag_{12}Au$ core. It is important to note that the Ag_{25} crystal structure[2] has three non-icosahedral Ag atoms out of the 12 atoms that face away from the triangular faces, while in $Ag_{24}Au$, all of these atoms were found to lie at the centers of the triangular faces. Similar to Ag_{25}, the Au-

doped clusters are also surrounded by six one-dimensional Ag_2S_3 motifs in a pseudo-O_h or a pseudo-T_h fashion, but the distortions (namely, strain) observed in the Ag_{25} motifs appear to be relieved after Au doping. Furthermore, the $Ag_{icosahedron}$–S and Ag_{motif}–S bond lengths in $Ag_{24}Au$ were slightly shortened (Supporting Information, Table S2) compared to those in Ag_{25}, which is suggestive of increased Ag–S bond strength. The effect of these subtle changes in the structure is reflected in the overall alloy cluster stabilities. Under ambient conditions, Au-doped clusters were found to be more stable for at least four days while the pure Ag_{25} showed signs of degradation after 24 hours (Supporting Information, Figure S7).

Further analysis of the $Ag_{24}Au(SPhMe_2)_{18}$ crystal structure reveals intermotif ligand interactions via phenyl rings of ligands (Figure 3A). Only eight out of 18 ligands were

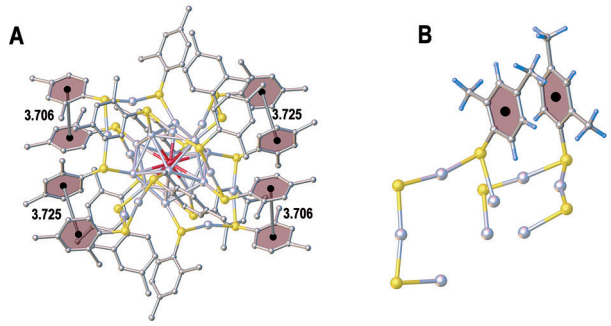

Figure 3. A) X-ray structure of $[Ag_{24}Au(SPhMe_2)_{18}]^-$, describing the intermotif interactions between motifs via π–π stacking of ligand phenyl rings. B) Orientation of ligands methyl groups in π–π interactions. Au red, Ag silver white, C gray, S yellow.[19]

observed to participate in π–π interactions (approximately face-to face, 3.706–3.725 Å) as opposed to 12 ligands in Ag_{25}.[2] The phenyl rings of the ligands involved in π–π interactions are oriented to keep the bulky methyl groups far apart to minimize repulsive interactions (Figure 3B). However, reasonable intermotif interactions via the Ag–S bond, similar to those found in Ag_{25},[2] could not be identified in the Au-doped clusters.

While the exact mechanism of doping of Ag_{25} with Au atoms is not clear, we speculate that the Au^+ ion is reduced to Au by Ag (upon reaching the core of Ag_{25} to form Ag^+) and replaces one of the icosahedron surface Ag atoms. The presence of the Au atom at this surface site may not be thermodynamically favorable, and therefore, Au diffuses to the core, pushing the central Ag atom to the surface. However, a theoretical study may be required to provide a definitive answer for the preferential diffusion of the atoms within the cluster.

To investigate the effect of heteroatom doping on the properties of Ag_{25} cluster, we synthesized an equivalent Pd-doped Ag_{25} cluster, $[Ag_{24}Pd(SPhMe_2)_{18}]^{2-}$, by following the original Ag_{25} synthesis (see the Supporting Information). It should be noted that Yan et al.[17] attained $[Ag_{24}Pd(SPhCl_2)_{18}]^{2-}$ through a similar method. ESI MS (Supporting Information, Figure S8) confirms the purity of our synthesized product and its charge state of 2−. The crystal structure of $[Ag_{24}Pd(SPhCl_2)_{18}]^{2-}$ was shown to contain a Pd atom at the center of Ag_{25}, similar to the Au in $[Ag_{24}Au(SPhMe_2)_{18}]^-$ in the case investigated in this study. The optical characterization of Ag_{25} and its alloy clusters with Au and Pd is shown in Figure 4. The $Ag_{24}Au$ cluster appears to be green to the

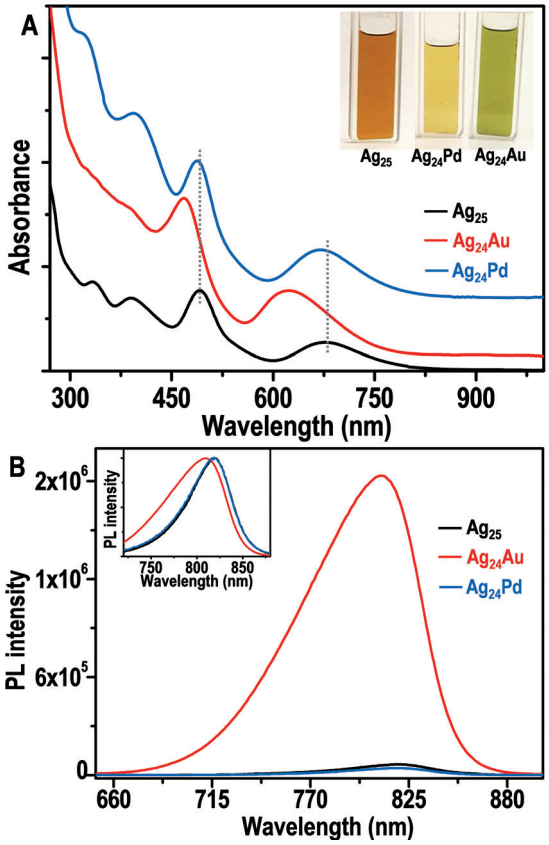

Figure 4. A) UV/Vis and B) photoluminescence spectra of $[Ag_{25}(SPhMe_2)_{18}]^-$, $[Ag_{24}Au(SPhMe_2)_{18}]^-$, and $[Ag_{24}Pd(SPhMe_2)_{18}]^{2-}$ clusters. The dotted lines show the peak shift relative to Ag_{25}. Inset of (A): Photographs of cluster solutions. The inset of (B): the shift in normalized photoluminescence spectra of Ag_{25} alloy clusters.

naked eye, while the $Ag_{24}Pd$ and pure Ag_{25} clusters are yellow and yellowish orange, respectively (Figure 4A inset). The absorption onset of Ag_{25} occurs at about 850 nm and is blue-shifted to about 800 and about 840 nm after doping with Au and Pd, respectively, along with a blue-shift of other major peaks (dotted lines in Figure 4A). The significant blue-shift (ca. 54 nm) in highest occupied molecular orbital to lowest unoccupied molecular orbital (HOMO–LUMO) gap[2,20] at 678 nm of Ag_{25} after doping with Au, unlike Pd-doping, illustrates the unique nature of the electronic perturbation owing to the incorporation of particular heteroatoms. We note that a similar blue-shift was reported for doped Au_{25} clusters.[9,11] The peaks at 390 and 334 nm in the $Ag_{24}Au$ are less pronounced compared to those of the parent Ag_{25} and $Ag_{24}Pd$; this may be due to the mixing of the Ag and Au electronic states,[16b] rendering these optical transitions forbidden in the $Ag_{24}Au$ cluster. The overall optical features of

the doped Ag_{25} clusters, except for the blue-shift of the peaks, are similar to those of pure Ag_{25}, indicating that the Ag_{25} structural framework is robust.

Additionally, we found that the photoluminescence of $Ag_{24}Au$ clusters was blue-shifted relative to those of pure Ag_{25} (Figure 4B inset), which are likely due to significant modulation in the HOMO–LUMO gap and/or in the surface states[21] after alloying. Interestingly, the luminescence of the Au-doped clusters was enhanced by a factor of ≥ 25 compared to that of pure Ag_{25} (Figure 4B); this may be attributed to the stabilization of the charges in the LUMO of the alloy cluster akin to $Au_{25-n}Ag_n$ cluster.[8,22] Conversely, we found a little change in the luminescence of $Ag_{24}Pd$ cluster.

We further characterized Ag_{25} and its alloy clusters using transient absorption (TA) spectroscopy with broadband capability to elucidate the excited-state properties. The experimental setup of TA is detailed elsewhere[23] (see also the Supporting Information). Upon optical excitation of Ag_{25} with a 350 nm laser pulse, we observed two ground-state bleaches (GSB) at 493 and 674 nm, corresponding to the Ag_{25} absorption bands, along with the two excited-state absorption bands at 450 and 570 nm (Figure 5A). Comparison of the transient spectra shows that for $Ag_{24}Pd$, a marginal shift in the GSB positions near 491 and 669 nm occurs, while the $Ag_{24}Au$ showed a larger spectral shift in the GSB position near 467 and 600 nm in accordance with their steady-state absorption (Figure 4A). These spectral shifts from Ag_{25} could be attributed to the modulation of the Ag_{25} electronic structure upon incorporation of the Pd and Au heteroatoms into the Ag_{25} structure. It was observed that a time window of 2.16 μs was sufficient for 100% decay in the excited-state absorption and full recovery in GSB of Ag_{25}. On the other hand, a > 4 μs time window was required for both excited-state absorption decay and GSB full recovery of Au-doped Ag_{25} (Supporting Information, Figure S9).

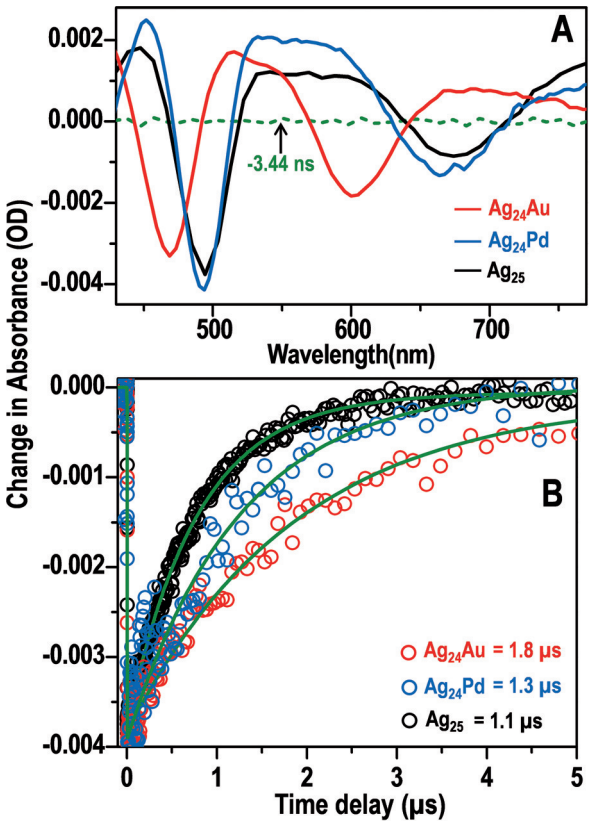

Figure 5. A) Transient absorption of $[Ag_{25}(SPhMe_2)_{18}]^-$, $[Ag_{24}Au(SPhMe_2)_{18}]^-$, and $[Ag_{24}Pd(SPhMe_2)_{18}]^{2-}$ clusters after optical excitation at 350 nm, at a time delay of 4 ns. B) Transient traces corresponding to the ground state bleach recovery from the spectra in (A). The solid green lines are fits of the kinetic traces.

The relaxation dynamics of the Ag_{25} alloy clusters were analyzed by fitting the time profiles representing the GSB with a single exponential decay function (Figure 5B). The time constant of the Ag_{25} excited-state decay of about 1.1 ± 0.1 μs may be due to a ligand-to-metal charge transfer state.[24] The relaxation time constant was found to increase for the Pd- and Au-alloyed Ag_{25} to approximately 1.3 and 1.8 μs, respectively. The presence of Pd and Au atoms in the Ag_{25} structure may change the excited charge state of the cluster owing to the modified electronic configuration, leading to longer relaxation time constants in the core- and ligand-localized charge-transfer type transitions.

In conclusion, we have designed and successfully synthesized a pure Au-doped $Ag_{25}(SR)_{18}$ cluster, $Ag_{24}Au(SR)_{18}$, by a novel galvanic exchange procedure. This method is compared with the direct synthesis, which produced a mixture of clusters. Optical spectroscopy, mass spectrometry, and single-crystal XRD analyses unambiguously confirmed the central Ag substitution of $[Ag_{25}(SR)_{18}]^-$ with the Au atom, forming a single nanoparticle composition $[Ag_{24}Au(SPhMe_2)_{18}]^-$ that preserves the structural framework of Ag_{25}. Heteroatom doping of Ag_{25} caused a significant increase in the material's stability and changes in electronic, optical, and luminescence properties. It is worth mentioning that $[Ag_{24}Au(SPhMe_2)_{18}]^-$ exhibited a 25-fold photoluminescence enhancement compared to $[Ag_{25}(SPhMe_2)_{18}]^-$. These model nanoparticles, namely Ag_{25}, $Ag_{24}Au$, and $Ag_{24}Pd$, will help elucidate the fundamental role of doping at the single-atom level. Such insights are critical for designing novel alloy nanoparticles with enhanced synergistic properties for applications in catalysis, energy, and sensing.

Acknowledgements

The authors acknowledge the use of KAUST resources.

Keywords: galvanic exchange · alloys · gold · silver · structure determination

How to cite: *Angew. Chem. Int. Ed.* **2016**, *55*, 922–926
Angew. Chem. **2016**, *128*, 934–938

[1] a) R. Jin, *Nanoscale* **2015**, *7*, 1549; b) A. Mathew, T. Pradeep, *Part. Part. Syst. Charact.* **2014**, *31*, 1017; c) K. Zheng, X. Yuan, N. Goswami, Q. Zhang, J. Xie, *RSC Adv.* **2014**, *4*, 60581; d) C. P. Joshi, M. S. Bootharaju, O. M. Bakr, *J. Phys. Chem. Lett.* **2015**, *6*, 3023; e) M. Huber, A. Schnepf, C. E. Anson, H. Schnöckel, *Angew. Chem. Int. Ed.* **2008**, *47*, 8201; *Angew. Chem.* **2008**, *120*, 8323.

[2] C. P. Joshi, M. S. Bootharaju, M. J. Alhilaly, O. M. Bakr, *J. Am. Chem. Soc.* **2015**, *137*, 11578.
[3] a) G. Li, D.-e. Jiang, S. Kumar, Y. Chen, R. Jin, *ACS Catal.* **2014**, *4*, 2463; b) L. G. AbdulHalim, M. S. Bootharaju, Q. Tang, S. Del Gobbo, R. G. AbdulHalim, M. Eddaoudi, D.-e. Jiang, O. M. Bakr, *J. Am. Chem. Soc.* **2015**, *137*, 11970.
[4] W. Kurashige, Y. Niihori, S. Sharma, Y. Negishi, *J. Phys. Chem. Lett.* **2014**, *5*, 4134, and references therein.
[5] a) H. Yang, Y. Wang, H. Huang, L. Gell, L. Lehtovaara, S. Malola, H. Häkkinen, N. Zheng, *Nat. Commun.* **2013**, *4*, 2422; b) A. Desireddy, B. E. Conn, J. Guo, B. Yoon, R. N. Barnett, B. M. Monahan, K. Kirschbaum, W. P. Griffith, R. L. Whetten, U. Landman, T. P. Bigioni, *Nature* **2013**, *501*, 399; c) O. M. Bakr, V. Amendola, C. M. Aikens, W. Wenseleers, R. Li, L. Dal Negro, G. C. Schatz, F. Stellacci, *Angew. Chem. Int. Ed.* **2009**, *48*, 5921; *Angew. Chem.* **2009**, *121*, 6035.
[6] a) T. Udayabhaskararao, Y. Sun, N. Goswami, S. K. Pal, K. Balasubramanian, T. Pradeep, *Angew. Chem. Int. Ed.* **2012**, *51*, 2155; *Angew. Chem.* **2012**, *124*, 2197; b) R. Jin, K. Nobusada, *Nano Res.* **2014**, *7*, 285; c) S. Wang, S. Jin, S. Yang, S. Chen, Y. Song, J. Zhang, M. Zhu, *Sci. Adv.* **2015**, *1*, e1500441.
[7] Y. Negishi, W. Kurashige, Y. Niihori, T. Iwasa, K. Nobusada, *Phys. Chem. Chem. Phys.* **2010**, *12*, 6219.
[8] S. Wang, X. Meng, A. Das, T. Li, Y. Song, T. Cao, X. Zhu, M. Zhu, R. Jin, *Angew. Chem. Int. Ed.* **2014**, *53*, 2376; *Angew. Chem.* **2014**, *126*, 2408.
[9] H. Qian, D.-e. Jiang, G. Li, C. Gayathri, A. Das, R. R. Gil, R. Jin, *J. Am. Chem. Soc.* **2012**, *134*, 16159.
[10] Y. Niihori, W. Kurashige, M. Matsuzaki, Y. Negishi, *Nanoscale* **2013**, *5*, 508.
[11] Y. Negishi, T. Iwai, M. Ide, *Chem. Commun.* **2010**, *46*, 4713.
[12] C. A. Fields-Zinna, M. C. Crowe, A. Dass, J. E. F. Weaver, R. W. Murray, *Langmuir* **2009**, *25*, 7704.
[13] L. Liao, S. Zhou, Y. Dai, L. Liu, C. Yao, C. Fu, J. Yang, Z. Wu, *J. Am. Chem. Soc.* **2015**, *137*, 9511.
[14] S. Wang, Y. Song, S. Jin, X. Liu, J. Zhang, Y. Pei, X. Meng, M. Chen, P. Li, M. Zhu, *J. Am. Chem. Soc.* **2015**, *137*, 4018.
[15] Y. Negishi, K. Munakata, W. Ohgake, K. Nobusada, *J. Phys. Chem. Lett.* **2012**, *3*, 2209.
[16] a) C. Kumara, C. M. Aikens, A. Dass, *J. Phys. Chem. Lett.* **2014**, *5*, 461; b) D. R. Kauffman, D. Alfonso, C. Matranga, H. Qian, R. Jin, *J. Phys. Chem. C* **2013**, *117*, 7914.
[17] J. Yan, H. Su, H. Yang, S. Malola, S. Lin, H. Häkkinen, N. Zheng, *J. Am. Chem. Soc.* **2015**, *137*, 11880.
[18] M. S. Bootharaju, V. M. Burlakov, T. M. D. Besong, C. P. Joshi, L. G. AbdulHalim, D. M. Black, R. L. Whetten, A. Goriely, O. M. Bakr, *Chem. Mater.* **2015**, *27*, 4289.
[19] CCDC 1429347 ($Ag_{24}Au$) contains the supplementary crystallographic data for this paper. These data can be obtained free of charge from The Cambridge Crystallographic Data Centre.
[20] C. M. Aikens, *J. Phys. Chem. C* **2008**, *112*, 19797.
[21] a) G. Wang, T. Huang, R. W. Murray, L. Menard, R. G. Nuzzo, *J. Am. Chem. Soc.* **2005**, *127*, 812; b) G. Wang, R. Guo, G. Kalyuzhny, J. P. Choi, R. W. Murray, *J. Phys. Chem. B* **2006**, *110*, 20282.
[22] M. Zhou, J. Zhong, S. Wang, Q. Guo, M. Zhu, Y. Pei, A. Xia, *J. Phys. Chem. C* **2015**, *119*, 18790.
[23] a) R. Bose, G. H. Ahmed, E. Alarousu, M. R. Parida, A. L. Abdelhady, O. M. Bakr, O. F. Mohammed, *J. Phys. Chem. C* **2015**, *119*, 3439; b) O. F. Mohammed, D. Xiao, V. S. Batista, E. T. J. Nibbering, *J. Phys. Chem. A* **2014**, *118*, 3090.
[24] a) S. H. Yau, O. Varnavski, T. Goodson, *Acc. Chem. Res.* **2013**, *46*, 1506; b) K. G. Stamplecoskie, Y. S. Chen, P. V. Kamat, *J. Phys. Chem. C* **2014**, *118*, 1370; c) M. Pelton, Y. Tang, O. M. Bakr, F. Stellacci, *J. Am. Chem. Soc.* **2012**, *134*, 11856.

Received: October 7, 2015
Published online: November 27, 2015

